2.N Nuclear Physics A280 (1977) 478–490; © North-Holland Publishing Co., Amsterdam

INTERACTIONS OF RELATIVISTIC NITROGEN NUCLEI IN AN EMULSION AT 2.1 GeV/NUCLEON

G. M. CHERNOV †, K. G. GULAMOV †, U. G. GULYAMOV, S. Z. NASYROV and L. N. SVECHNIKOVA †

Institute of Nuclear Physics, Uzbek SSR Academy of Sciences, Ulugbek, 702132, USSR

Received 12 August 1976
(Revised 13 December 1976)

Abstract: An analysis of multiple production induced by 2.1 GeV/n ^{14}N ions in nuclear emulsions is presented. Multiplicity and angular distributions of charged secondaries and correlations among them are discussed. The presented data are compared with relevant values from proton-nucleus interactions. The possible appearence of collective phenomena in nucleus-nucleus interactions is discussed.

E NUCLEAR REACTIONS Ag, Br, N, O, C(^{14}N, X), E = 2.1 GeV/nucleon; measured multiplicities, angular distributions, deduced multiplicities of projectile fragments, asymmetry and coplanarity coefficients, the upper limit of σ for nuclear shock waves.

1. Introduction

The recent availability of relativistic nuclear beams at the Lawrence Berkeley Laboratory and Joint Institute for Nuclear Research makes it interesting to study various aspects of nucleus-nucleus interactions at high energies and opens a new area for physics research – relativistic nuclear physics [1,2]). The main part of inelastic nucleus-nucleus cross section at high energies is conditioned by multiple production and we will discuss in the present paper some general features of such processes in collisions of ^{14}N ions with emulsion nuclei.

2. Experimental details

A stack of 600 μm thick Ilford G-5 nuclear emulsions was exposed to the T = 2.1 GeV/nucleon ^{14}N beam at the Berkeley Bevatron. By double, fast and slow, "along the track" scanning 1813 inelastic nitrogen interactions were recorded along the total length of 247 m, leading to the mean free path for inelastic interaction $\lambda = 13.6 \pm 0.4$ cm. In all, 504 ^{14}N emulsion (NA) events selected without any discrimination were used for angular measurements and further analysis. All charged

† Also at the Physical Technical Institute, Tashkent, USSR.

secondaries in these events were classified, in accordance with the emulsion terminology, into the following types:

(a) black (b) particles with the range $L < 3$ mm;

(b) gray (g) particles with $L > 3$ mm and ionization $g/g^0 > 1.4$, where g^0 is the plateau grain density for singly charged particles, except particles of type (d) (see below);

(c) relativistic (s) particles with $g/g^0 < 1.4$;

(d) doubly charged fragments of the projectile with a constant $g/g^0 \approx 4$ along the track length of 2 cm ionization, and $\theta < 5°$ (θ is the emission angle in the lab frame);

(e) multiply charged ($Z \geqq 3$) projectile fragments with a constant $g/g^0 > 7$ along the length of 2 cm ionization, and $\theta < 5°$.

The heavily ionizing particles (h-particles, $n_h = n_b + n_g$) of types (a) and (b) come from the target; particles (d) and (e) belong to the projectile; and s-particles contain the particles produced, single charged relativistic recoils from target and single charged fragments of projectile. We chose the noninteracting single charged projectile fragments from s-particles (see subsect. 3.2) and hereafter the relativistic particles without such fragments will be designated as s′ particles.

3. Multiplicity and angular distributions

3.1. MULTIPLICITIES OF CHARGED PARTICLES

The mean multiplicities of different secondary particles from NA collisions in comparison with proton-emulsion (pA) data at the nearby energy $T = 2.23$ GeV [ref. [3])] are presented in table 1. As one can see, the multiplicity of relativistic particles in NA collisions is larger by almost an order of magnitude than in pA interactions and the multiplicity of gray particles more than doubles; it is interesting that

TABLE 1

A comparison of the mean multiplicities in NA and pA interactions

	NA $T = 2.1$ GeV/n	pA [a]) $T = 2.23$ GeV
Number of events	504	702
$\langle n_s \rangle$	8.85 ± 0.28	0.95 ± 0.05
$\langle n_{s'} \rangle$	7.70 ± 0.29	0.95 ± 0.05
$\langle n_g \rangle$	5.29 ± 0.31	2.42 ± 0.12
$\langle n_b \rangle$	4.57 ± 0.21	4.45 ± 0.22
$\langle n_{Z=1} \rangle$	1.15 ± 0.05	
$\langle n_{Z=2} \rangle$	0.81 ± 0.04	
$\langle n_{Z \geq 3} \rangle$	0.17 ± 0.02	

[a]) Ref. [3]).

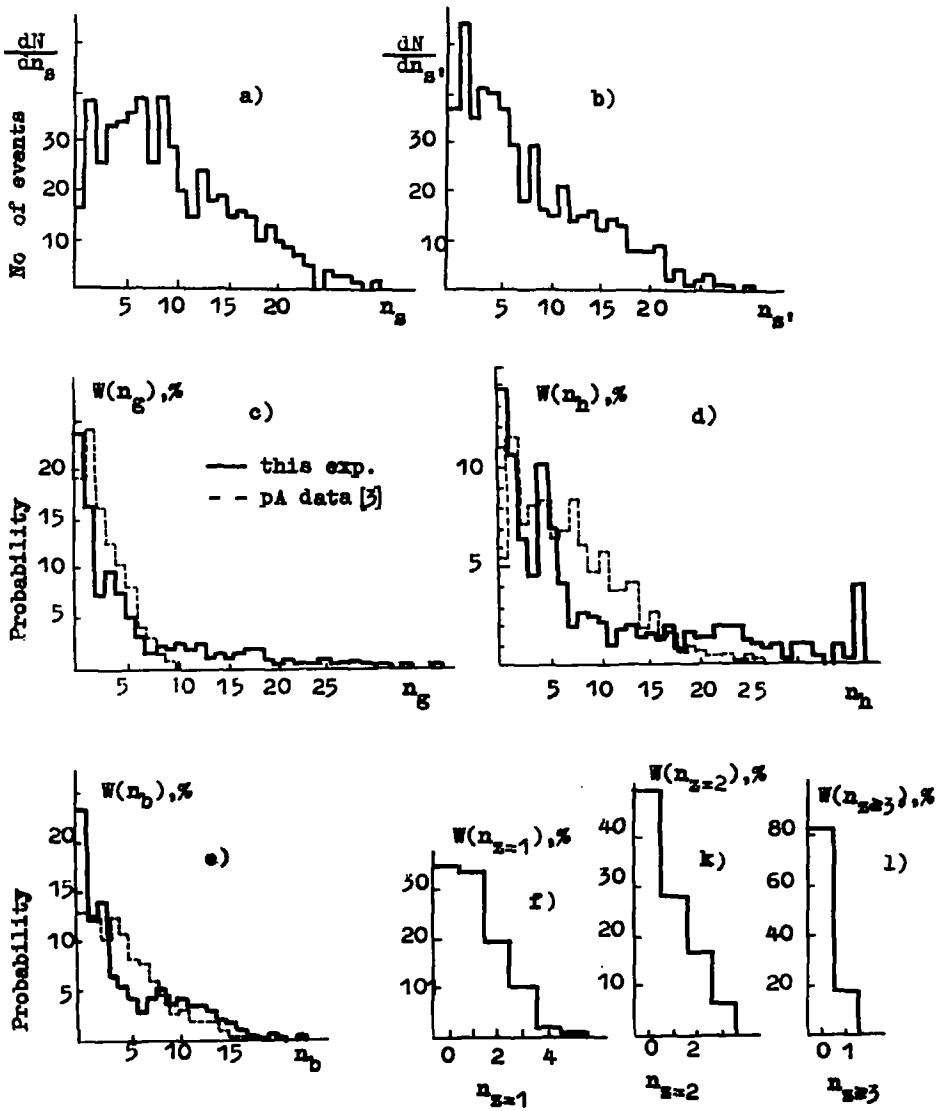

Fig. 1. Multiplicity distributions of different types of charged secondaries in NA interactions. The dotted histograms represent pA data [3]).

the mean number of b-particles does not change within errors, showing the approximate equality of the residual nucleus excitations in NA and pA collisions.

Multiplicity distributions in NA and pA interactions are plotted in fig. 1. One can note that:

(i) Although $\langle n_b \rangle$ is the same both in NA and pA collisions, the shapes of n_b distributions are different: the n_b distribution for NA events is enriched by the small and large n_b.

(ii) The n_g distribution in NA interactions has a tail up to $n_g = 33$ and differs significantly from that in pA collisions.

(iii) There is the well-expressed minimum (dip) in the n_h distribution for NA events at $n_h \approx 2$–3.

3.2. ANGULAR DISTRIBUTIONS

The angular distributions of b- and g-particles in NA interactions are shown in fig. 2. For comparison purposes we have plotted there also the angular spectra from pA collisions [3]). We see that there is no dependence of those distributions on the atomic number of projectile. This fact may be considered as an indication that the heavy particle production mechanism is probably of the same nature in NA and pA

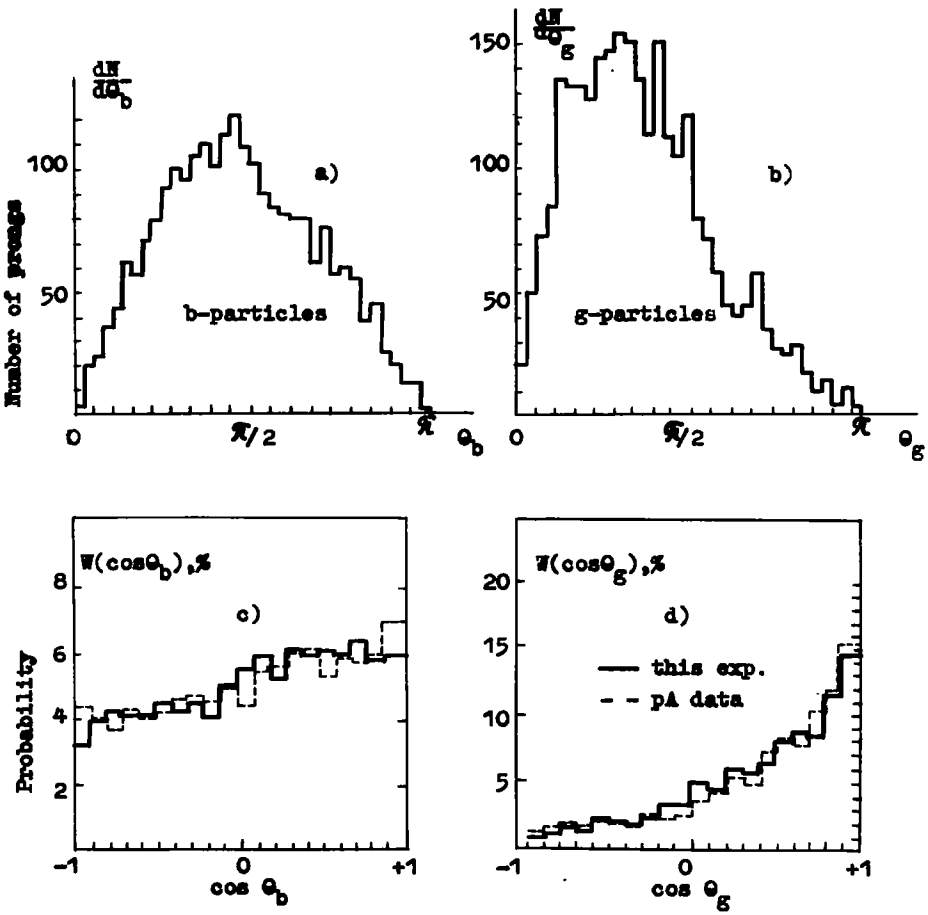

Fig. 2. Angular distributions of heavily ionizing particles in NA collisions. The dotted histograms give the pA data.

interactions. We note, of course, that although the angular spectra of the target fragments are anisotropic, they have smooth shapes without any narrow peaks.

In figs. 3a and b the angular distributions of s′ particles are compared with the corresponding pA data and fig. 3c shows the angular distribution of s-particles in the range of the smallest angles. In this range ($1 \geqq \cos\theta \gtrsim 0.99$) the angular distribution of relativistic particles in pA interactions is close to the uniform one (the dotted line in fig. 3c), while NA events demonstrate the pronounced peak at $\cos\theta = 1$.

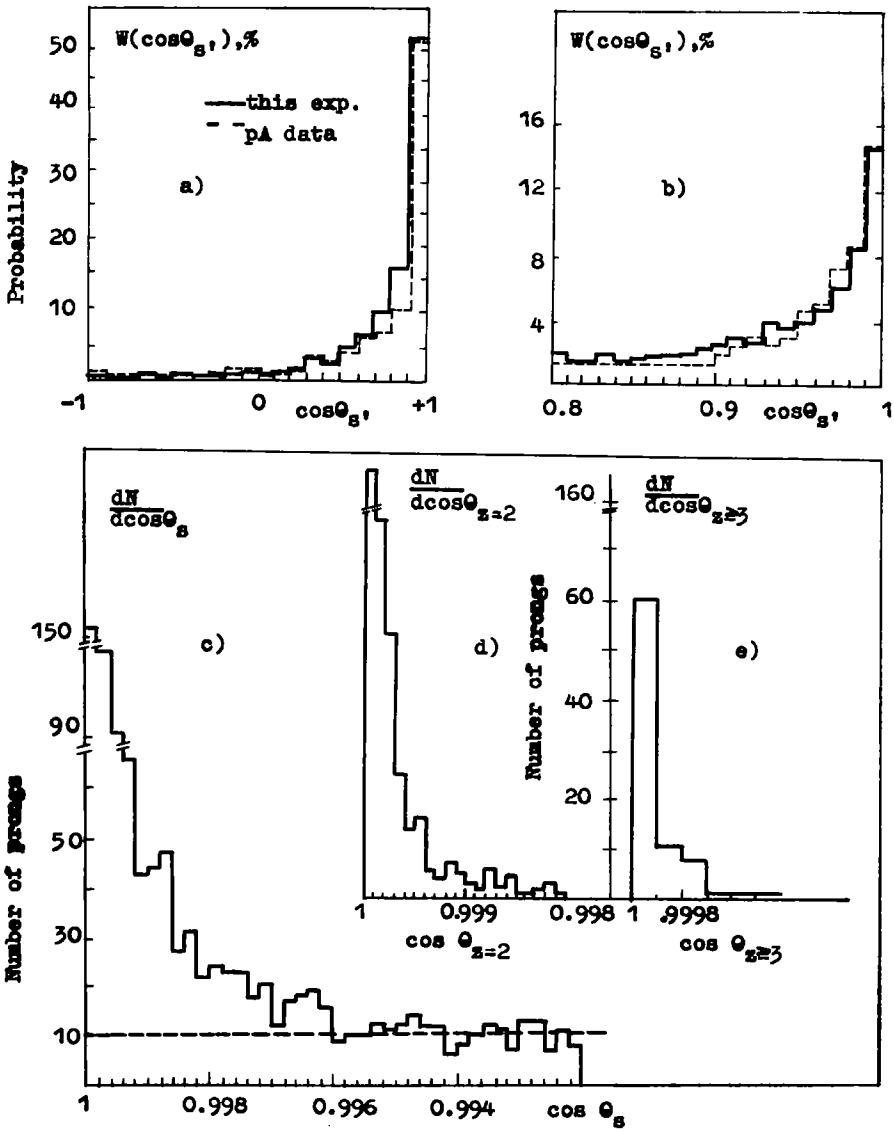

Fig. 3. Angular distributions of relativistic particles in NA and pA interactions.

It is natural to assume that this forward peak is caused by noninteracting single charged fragments of the projectile (see, for comparison figs. 3d and e, where we have plotted the angular distributions of well identified projectile fragments having $Z \geqq 2$). Then the elementary subtraction procedure performed in the region $\cos\theta > 0.996$ (fig. 3c) gives us their angular distribution and multiplicity.

Comparing the data from figs. 3c–e one can conclude that the larger projectile fragment, the narrower angular distributions – the well known result observed earlier in cosmic ray experiments [4]).

3.3. DEPENDENCE OF MULTIPLICITY AND ANGULAR SPECTRA ON THE NUMBER OF INTERACTING PROJECTILE NUCLEONS

The number of projectile nucleons interacting with the target (m) is one of the basic parameters of the so called superposition model, where a nucleus-nucleus interaction is described as a superposition of nucleon-nucleus collisions [5,6]). Therefore it is attractive to study the dependence of several characteristics of multiple production on this quantity. A crude estimate of the value of m can easily be obtained from the relation $m = 14 - 2Q$, where Q is the total charge of noninteracting projectile fragments. The "minimal" value of Q is $Q^{\min} = n_{Z=1} + 2n_{Z=2} + 3n_{Z\geqq 3}$ (n_Z is the number of fragments with fixed Z; at $Q^{\min} = 2$, $Q^{\min} = Q$). Therefore we will use for a crude classification of NA interactions the quantity

$$m = \begin{cases} 1, & \text{if } Q^{\min} \geqq 7 \\ 2(7 - Q^{\min}), & \text{if } Q^{\min} < 7. \end{cases} \tag{1}$$

Bearing in mind the data on $\langle n_Z \rangle$ from table 1, it is easy to determine the average number of interacting nucleons (or more exactly, the upper limit of this quantity) in nitrogen-emulsion collisions as

$$\langle m \rangle = 7.34. \tag{2}$$

It should be noted that our result is in excellent agreement with the value obtained recently [6]) from an analysis of cosmic ray data.

In fig. 4 we present the dependence of the mean multiplicities of different types of particles and some parameters of the angular distributions [the average values of the quasirapidity $\eta = -\ln(\tan \frac{1}{2}\theta)$ and dispersions of η-spectra] on m. We see that:

(i) The mean multiplicities of all types of secondaries increase monotonically with m; for $\langle n_{s'} \rangle$ this growth is close to the linear one. The "relative multiplicities" of relativistic particles $\langle n_s \rangle / m$ are approximately identical and close to the $\langle n_s \rangle$ in pA interactions at the same energy (see fig. 4b).

(ii) The angular distributions of s′ particles depend rather weakly on m (figs. 4e and f).

It should be noted that in fig. 4 one observes a change in the slope of the m-dependence at $m \approx 8$, which can be explained (at least partially) by an underestimation

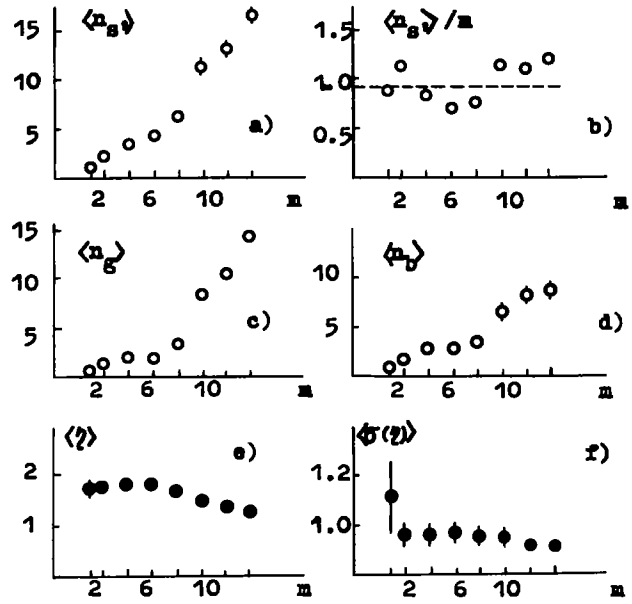

Fig. 4. Mean multiplicities of secondary particles (a–d); the mean quasirapidity (e), and dispersion $\sigma(\eta)$ of η-spectra (f) as functions of the number of interacting projectile nucleons.

of the charges of multicharged ($Z \geqq 3$) fragments from the projectile nucleus. In fact, there is a considerable number of events having only one multicharged fragment and very small multiplicities of secondaries in the region $m = 6$–8. Really these events belong to smaller m.

The data considered do not contradict the assumption that, in the first approximation, nucleus-nucleus interactions at energies ≈ 2 GeV/nucleon can be considered as a superposition of "elementary" nucleon-nucleus collisions.

4. Two-particle correlations among secondaries

Additional information on the mechanism of nucleus-nucleus interactions can be obtained from an investigation of correlations between secondary particles. In particular, it is possible to draw more certain conclusions on collective phenomena such as nuclear shock waves and high angular momentum transfer to the reaction products.

4.1. LONGITUDINAL CORRELATIONS AND NUCLEAR SHOCK WAVES

The idea that a nuclear shock wave could be produced when a high energy particle moves through a nucleus was proposed by Glassgold, Heckrotte and Watson [7]). After this several concrete theoretical models were suggested for nuclear shock waves

[refs. [8-13])], although this is by no means implies that the hydrodynamic approximation is applicable to the collisions of objects containing as few particles as atomic nuclei [14,15]). The common prediction of all these models is the preferential emission of target fragments in the direction perpendicular to the Mach shock front. Unfortunately, the experimental data are poor and the real situation seems to be unclear [16-18]).

Our experimental data (see fig. 2) demonstrate the absence of any singularity in the angular distributions for the target fragments. It is obvious that due to the composite nature of emulsion containing a mixture of nuclei (Ag, Br, O, N, C), one cannot claim the absence of nuclear shock waves. In general, we believe, it is very difficult to obtain reliable information on such phenomena from the one-particle distributions alone.

Therefore we propose here an analysis by means of methods sensitive to the generation of shock waves in individual collisions. In the ideal case, when the well-defined Mach cone is developed, one can observe the preferential emission of nuclear matter. We would like to stress that such emissions must lead to the "short-range" angular correlations among secondaries. It is very important that in practice, when the Fermi motion of intranuclear nucleons spreads out the Mach cone, the short-ranged nature of correlations will be conserved [in accordance with calculations [13]) the Fermi motion gives deviations of $\approx 20°$, i.e. ≈ 0.05 of the whole $\cos\theta$ interval].

At first we will use the standard correlation functions

$$C_2(z_1, z_2) = \frac{1}{\sigma_{\text{in}}} \frac{\mathrm{d}^2\sigma}{\mathrm{d}z_1 \mathrm{d}z_2} - \frac{1}{\sigma_{\text{in}}^2} \frac{\mathrm{d}\sigma}{\mathrm{d}z_1} \frac{\mathrm{d}\sigma}{\mathrm{d}z_2}, \tag{3}$$

$$R_2(z_1, z_2) = \sigma_{\text{in}} \frac{\mathrm{d}^2\sigma}{\mathrm{d}z_1 \mathrm{d}z_2} \Big/ \frac{\mathrm{d}\sigma}{\mathrm{d}z_1} \frac{\mathrm{d}\sigma}{\mathrm{d}z_2} - 1, \tag{4}$$

where z equals $\cos\theta$ for g- and b-particles and $z = \eta = -\ln(\tan \frac{1}{2}\theta)$ for relativistic particles, respectively. Since the broad multiplicity distribution and the dependence of the one-particle spectrum $\mathrm{d}\sigma/\mathrm{d}z$ on the multiplicity lead to the trivial and rather strong pseudocorrelations, we calculated the correlation functions by the Monte Carlo method under the following assumptions:

(a) Particles of all types are emitted independently of each other.

(b) The angular distributions of all types of particles coincide exactly with the empirical "semi-inclusive" (i.e. at fixed n_s, n_b and n_g) one-particle distributions.

(c) Multiplicity distributions coincide with the empirical spectra.

The experimental data on $C_2(z_1, z_2)$ and $R_2(z_1, z_2)$, and the solid curves corresponding to the described model are presented in figs. 5 and 6. For b- and g-particles only $C_2(z_1, z_2)$ are shown since $R_2(z_1, z_2)$ gives similar results. In order to investigate the influence of nuclear shock waves on the correlation functions additional calculations have been performed. In these calculations we used the following angular distributions: (i) the angular distribution of g-particles taken from the hydrodynamic

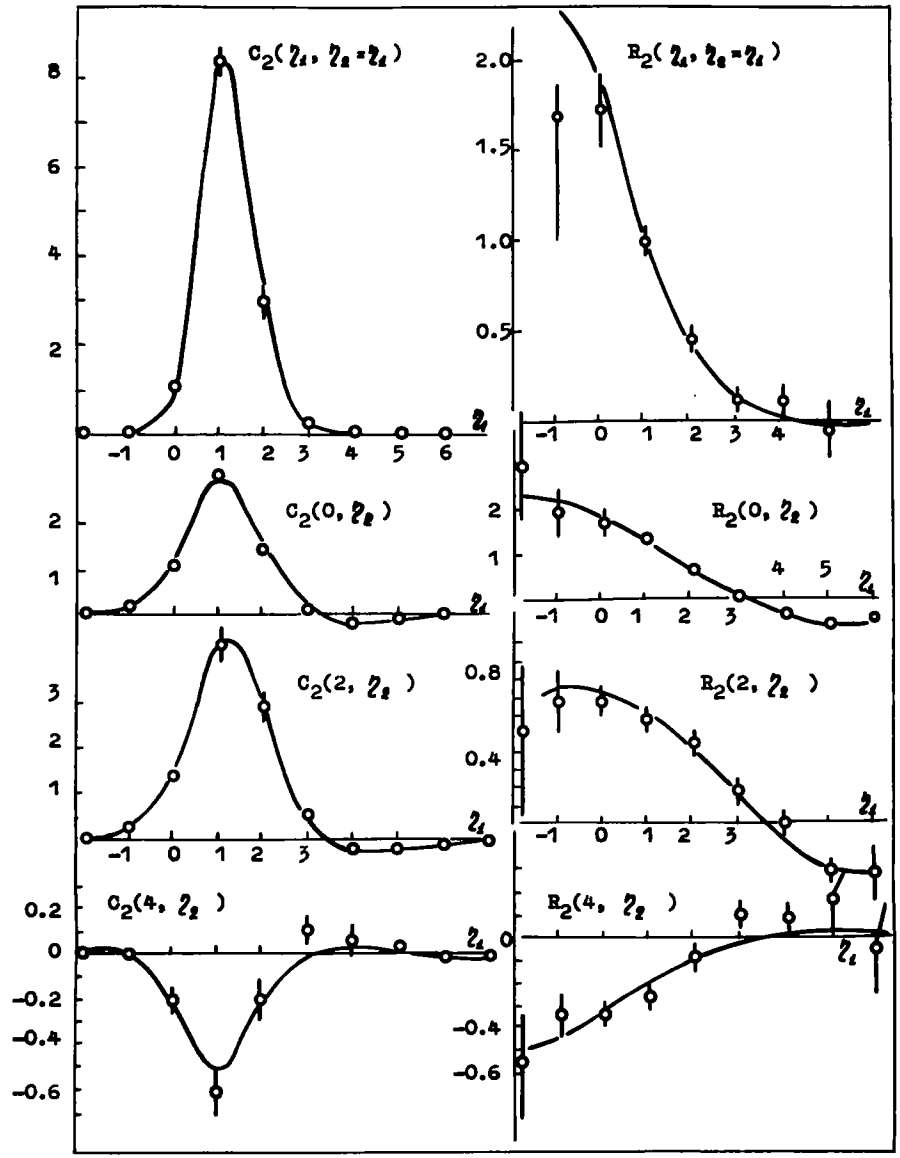

Fig. 5. Two-particle correlation functions $C_2(\eta_1, \eta_2)$ and $R_2(\eta_1, \eta_2)$ for relativistic particles in NA interactions. The curves are the predictions of the independent emission model.

model [12]), (ii) the angular distribution of b-particles from the interactions of 2.1 GeV/n ^{16}O ions with AgCl [ref. [16])], and (iii) the uniform angular distributions for b- and g-particles considered as the "background".

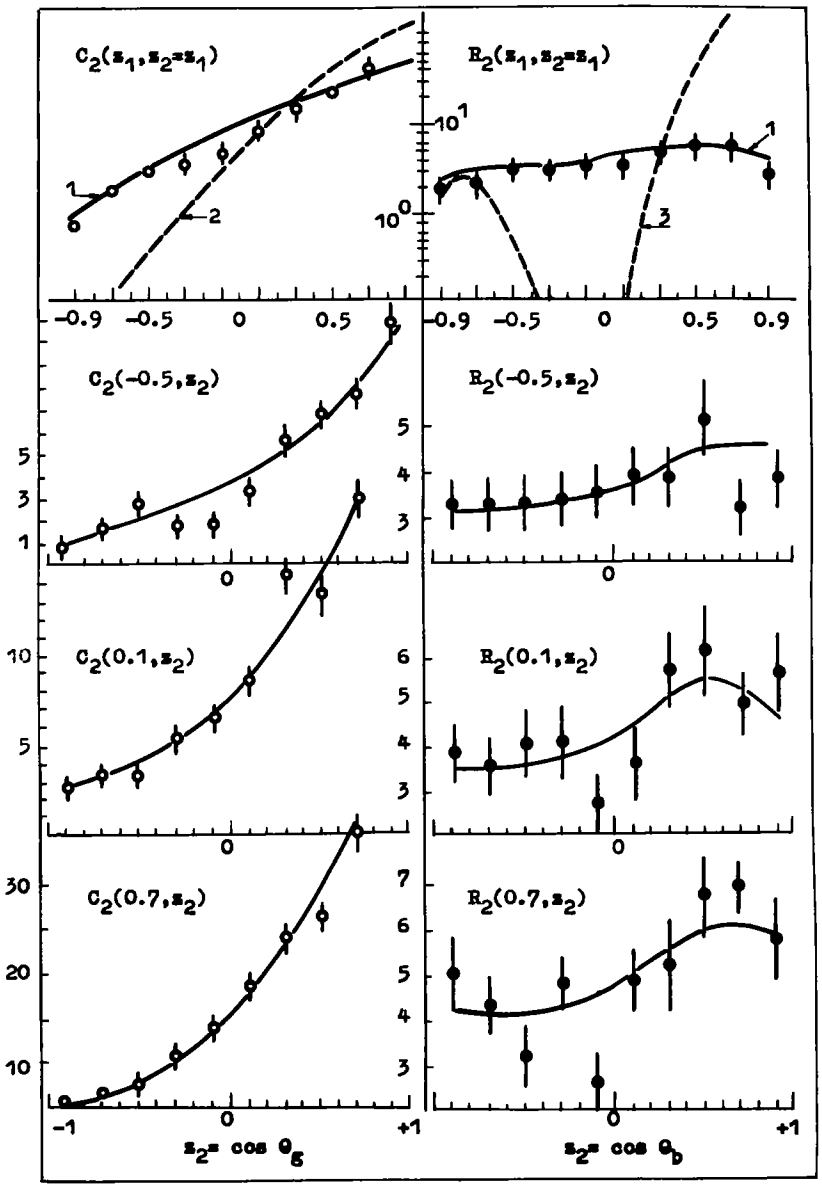

Fig. 6. The correlation function $C_2(\cos\theta_1, \cos\theta_2)$ for black (the right half of the figure) and gray (the left half) particles. The solid curves are the independent emission model predictions; curve 2 corresponds to the hydrodynamic model [12]) and the curve 3 to the angular distribution from ref. [16]).

The results of these calculations are represented in figs. 5–7; by the curves 2, 3 and the dotted histograms, respectively.

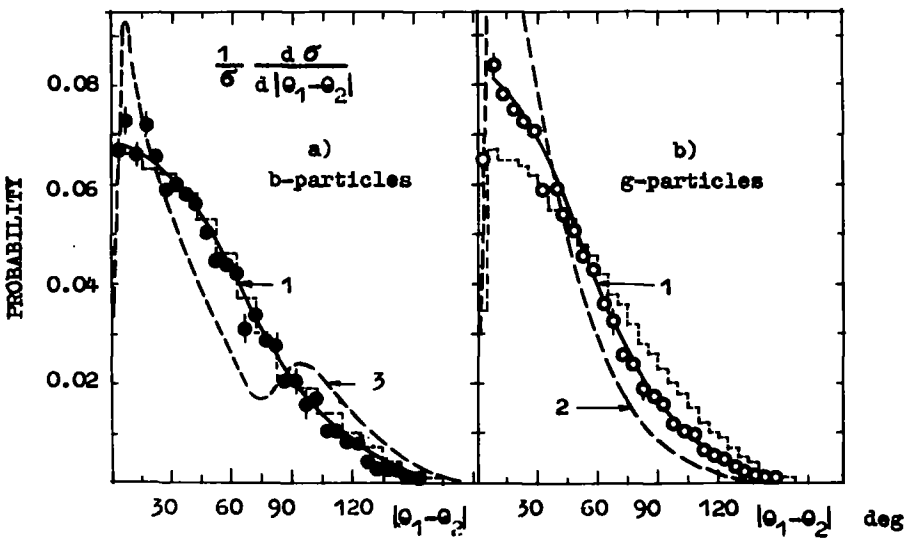

Fig. 7. The function $(1/\sigma)(d\sigma/d|\theta_1-\theta_2|)$ versus $|\theta_1-\theta_2|$ for b- and g-particles. For curves and dotted histograms see text and fig. 6.

From figs. 5 and 6 one can conclude that:

(i) The experimental data agree fairly well with the hypothesis of independent emission of all types of particles in NA interactions.

(ii) The absence of noticeable short-range correlations between the target fragments (see the values of the function C_2 at $z_1 = z_2$) contradicts the assumption of shock wave generation in the larger part of NA collisions.

(iii) Our data disagree with the model predictions of ref. [12]).

In fig. 7 we show the distributions of the quantity $(1/\sigma)(d\sigma/d|\theta_1-\theta_2|)$ for black and grey particles from NA interactions. The preferable emission of nuclear fragments at any angle in individual collisions will manifest itself as a "singularity" in this distribution. It is seen from fig. 7 that the experimental data are in a good agreement with the independent emission model. The experimental data for b-particles are close to the background histogram, whereas the data for g-particles show some deviation at $\Delta\theta < 35°$. It is obvious that this deviation is caused by the above-mentioned anisotropy of the g-particle angular distribution, which, in turn, could be due to several physical reasons (particularly to the quasielastic scattering). It is easy to define the upper limit of the cross section for nuclear shock wave production if one assumes that this enhancement is caused by shock waves. Then, by subtraction of the background from the experimental distribution in the region $\Delta\theta < 35°$, one can obtain

$$\sigma_{max}(\text{shock waves}) \lesssim 0.05\sigma_{inel}(\text{NA}). \tag{5}$$

4.2. AZIMUTHAL CORRELATIONS

A study of correlations in the azimuthal plane can give useful information on the mechanism of production; in particular, the high angular momentum transferred to the produced particles will lead to large values of the coplanarity coefficients.

TABLE 2

Asymmetry and coplanarity coefficients for different types of charged particles in NA interactions

Type of particles	A	B
s	0.003 ± 0.006	-0.009 ± 0.006
s′	0.007 ± 0.007	-0.008 ± 0.007
g	-0.003 ± 0.008	0.026 ± 0.008
b	0.001 ± 0.010	-0.006 ± 0.010
projectile fragments with $Z = 1$	-0.070 ± 0.053	-0.048 ± 0.053
projectile fragments with $Z = 2$	-0.006 ± 0.074	0.028 ± 0.074
all projectile fragments ($Z \geq 1$)	-0.031 ± 0.030	-0.013 ± 0.030

Table 2 presents the values of the asymmetry

$$A = \left(\int_{\frac{1}{2}\pi}^{\pi} \frac{d\sigma}{d\varepsilon} d\varepsilon - \int_{0}^{\frac{1}{2}\pi} \frac{d\sigma}{d\varepsilon} d\varepsilon \right) \Big/ \int_{0}^{\pi} \frac{d\sigma}{d\varepsilon} d\varepsilon, \tag{6}$$

and the coplanarity

$$B = \left(\int_{0}^{\frac{1}{2}\pi} \frac{d\sigma}{d\varepsilon} d\varepsilon - \int_{\frac{1}{2}\pi}^{\frac{1}{2}\pi} \frac{d\sigma}{d\varepsilon} d\varepsilon + \int_{\frac{1}{2}\pi}^{\pi} \frac{d\sigma}{d\varepsilon} d\varepsilon \right) \Big/ \int_{0}^{\pi} \frac{d\sigma}{d\varepsilon} d\varepsilon, \tag{7}$$

coefficients of the ε-distribution, where ε is the angle between the transverse momenta of the particles considered and $\varepsilon = \arccos(\boldsymbol{p}_{1\perp}\boldsymbol{p}_{2\perp})/|\boldsymbol{p}_{1\perp}\boldsymbol{p}_{2\perp}|$. The data show that these coefficients do not contradict the zeroth values, i.e. do not display any correlation effects.

It should be noted, of course, that momentum conservation leads to positive A-values (just as in hadron-hadron interactions). Therefore having experimental values of A equal to zero for relativistic particles indicates that the conservation laws have been "dropped" from the particles' memory. Thus, it is additional evidence confirming the independence of relativistic particles (i.e. the cascade mechanism).

5. Conclusions

The main conclusions drawn from this investigation are summarised below:

(i) The data on multiplicity and angular spectra from nitrogen-emulsion interactions at 2.1 GeV/nucleon and their dependence on the number of interacting projectile nucleons do not contradict the cascade model.

(ii) The angular distributions of the target fragments depend on the atomic number of projectile only very weakly.

(iii) The role of collective phenomena such as nuclear shock waves and high angular momentum transfer is very small in NA interactions.

Thus, we confirm experimentally the hypothesis [14]) that heavy ions collisions at energies of about a few GeV/n resemble more gases passing through each other than droplets splashing on each other.

We are glad to express our sincere gratitude to Prof. H. H. Heckman for the allotment of the emulsion stack irradiated at the LBL. The friendly help of Dr. A. I. Bondarenko in this work is greatly appreciated and we thank Dr. B. S. Yuldashev and Mrs. A. F. Zakatej for the careful reading of the manuscript and useful comments.

References

1) H. H. Heckman, Lawrence Berkeley Laboratory report LBL-2052 (1973)
2) A. M. Baldin, Joint Institute for Nuclear Research report E-9138 (1975)
3) M. Bogdanski *et al.*, Helv. Phys. Acta **42** (1969) 485
4) C. F. Powell, P. H. Fowler and D. H. Perkins, The study of elementary particles by the photographic method (Pergamon Press, New York, 1959) chap. 16
5) R. Kullberg *et al.*, Phys. Scripta **5** (1972) 5
6) A. Tomassewski and J. Wdowczyk, J. of Phys. **A8** (1975) 1189
7) A. Glassgold *et al.*, Ann. of Phys. **6** (1959) 1
8) W. Greiner, Proc. Summer Study on high energy heavy ions, Berkeley, 1974, ed. L. S. Schroeder (LBL-3675, Berkeley, 1975) p. 1;
W. Scheid *et al.*, Phys. Rev. Lett. **32** (1974) 741
9) C. Y. Wong and T. A. Welton, Phys. Lett. **49B** (1974) 243
10) Y. Kitasoe and M. Sano, Osaka Univ. report OULNS 75-6 (1975)
11) M. I. Sobel *et al.*, Nucl. Phys. **A251** (1975) 502
12) A. A. Amsden *et al.*, Phys. Rev. Lett. **35** (1975) 905
13) B. A. Rumyantzev, ZhETF Pizma **22** (1975) 114;
B. A. Rumyantzev *et al.*, ZhETF Pizma **23** (1976) 309
14) G. F. Bertsch, Phys. Rev. Lett. **34** (1975) 697
15) G. Chapline, Lawrence Livermore Laboratory report UCRL – 76065 (1974)
16) H. G. Baumgardt *et al.*, Z. Phys. **A273** (1975) 359
17) L. P. Remsberg and D. G. Perry, Phys. Rev. Lett. **35** (1975) 361
18) A. M. Poskanzer *et al.*, Phys. Rev. Lett. **35** (1975) 1701